

Structural and dielectric studies of the phase behaviour of the topological ferroelectric $\text{La}_{1-x}\text{Nd}_x\text{TaO}_4$

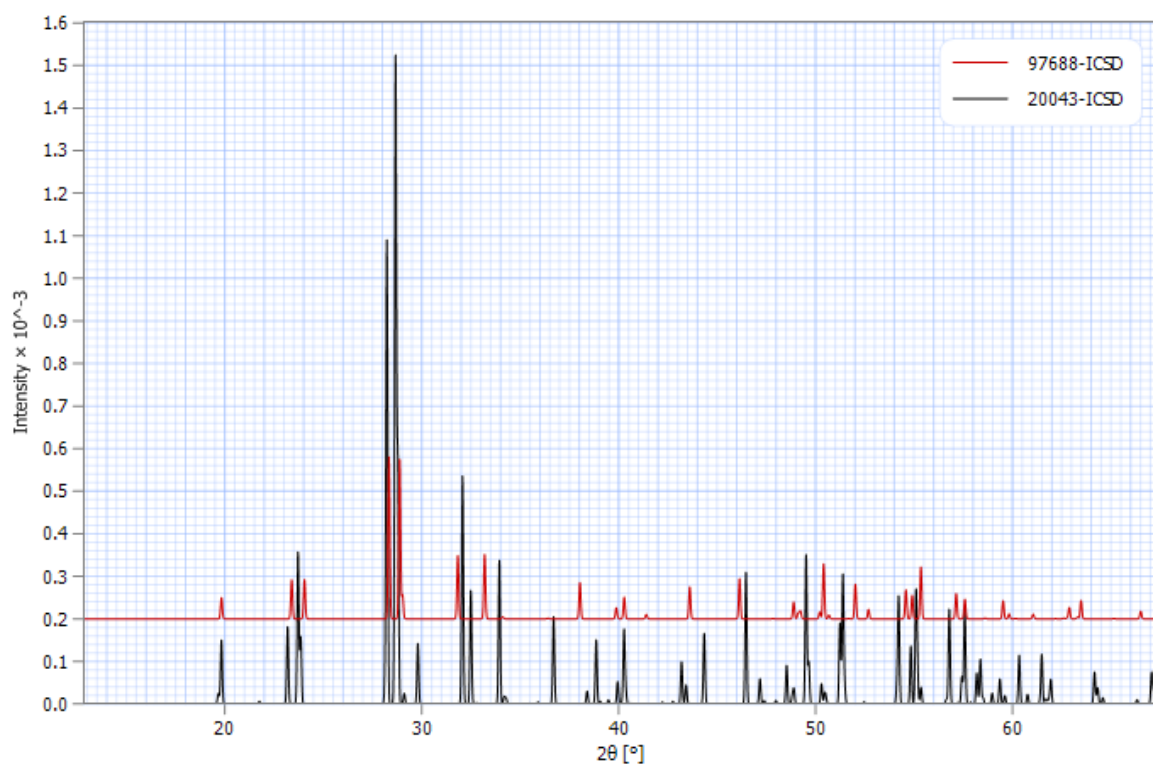
Keith J. Cordrey¹, Magda Stanczyk¹, Charlotte A. L. Dixon¹, Kevin S. Knight², Jonathan Gardner¹, Finlay D. Morrison¹ and Philip Lightfoot^{1*}

1. EaStCHEM and School of Chemistry, University of St Andrews, St Andrews, Fife, KY16 9ST, UK.
2. ISIS Facility, STFC Rutherford Appleton Laboratory, Harwell, Oxfordshire, OX11 0QX, UK.

*Corresponding author, e-mail: pl@st-and.ac.uk

SUPPLEMENTARY MATERIAL

Figure S1. Standard powder XRD patterns (CuK_α radiation) for O-LaTaO₄ (top curve, red; Cava et al., ICSD 97688) and M-LaTaO₄ (bottom curve, black; Kurova et al., ICSD 20043). Simulations generated using CrystalDiffract® software.



Rietveld analysis of O-LaTaO₄ NPD data

Refinements were carried out using the same set of refined variables at each temperature. For O-LaTaO₄, 37 variables were refined: 2 scale, 1 diffractometer constant, 8 background and 6 peak-shape parameters for the two histograms, 3 lattice parameters, 11 xyz, 6 Uiso. Final refinement details at 100 and 500 °C are given in cif format; selected bond lengths are given below:

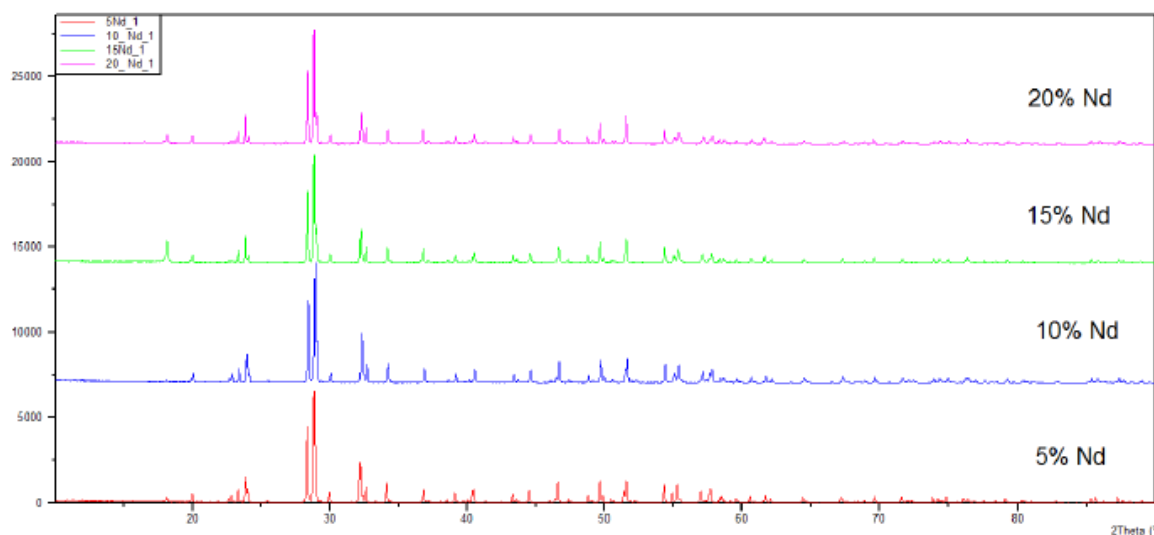
Table S1. Metal-oxygen bond distances for O-LaTaO₄ at 100 and 500 °C

	<u>100 °C</u>	<u>500 °C</u>
Ta – O1	2.016(5)	2.036(4)
Ta – O2	1.911(4)	1.891(4)
Ta – O3	1.918(4)	1.927(4)
Ta – O3	2.078(5)	2.093(4)
Ta – O4 (x 2)	1.981(6)	1.983(5)
La – O1	2.400(6)	2.392(5)
La – O1' (x 2)	2.491(4)	2.495(3)
La – O2 (x 2)	2.481(3)	2.508(3)
La – O2	2.770(5)	2.813(5)
La – O3 (x 2)	2.923(3)	2.899(3)
La – O4	2.696(5)	2.723(4)

Rietveld analysis of M-La_{1-x}Nd_xTaO₄ XPD data

A fixed structural model was used, with only background, peak shape, an overall thermal parameter, and lattice parameters being refined. Raw data plots and refined lattice parameters are given below:

Figure S2. Raw XPD data for M-La_{1-x}Nd_xTaO₄ showing solid solution formation for 0 < x < 0.40, and presence of a secondary phase (fergusonite polymorph) for x > 0.40.



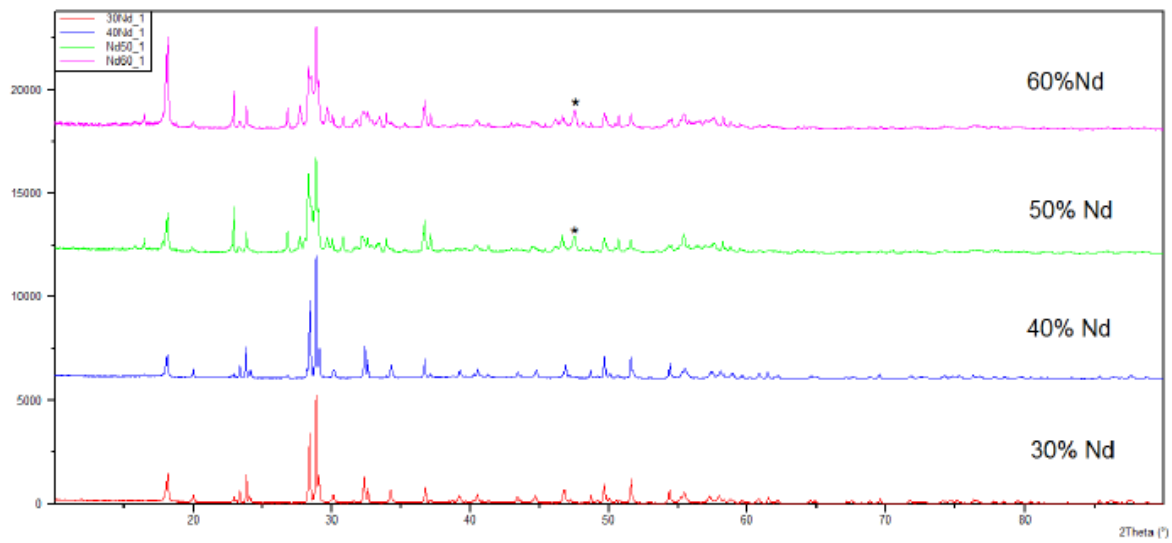


Table S2. Refined lattice parameters for M-La_{1-x}Nd_xTaO₄ from XPD.

x	a (Å)	b (Å)	c (Å)	β (deg)	V (Å ³)
0.05	7.63193(9)	5.57599(7)	7.81983(9)	101.460(1)	326.144(5)
0.10	7.6317(1)	5.5702(1)	7.8140(1)	101.374(1)	325.65(1)
0.15	7.6296(1)	5.5652(1)	7.8079(1)	101.313(1)	325.09(1)
0.20	7.6277(1)	5.5575(1)	7.7992(1)	101.211(1)	324.31(1)
0.30	7.6248(2)	5.5473(1)	7.7875(2)	101.077(2)	323.26(2)
0.40	7.6194(2)	5.5344(1)	7.7728(2)	100.914(2)	321.85(2)

Rietveld analysis of O-/M-La_{0.9}Nd_{0.1}TaO₄ NPD data

As for the O-LaTaO₄ refinements a consistent set of profile parameters were refined at each temperature. For single phase refinements at 100 – 200 °C (M-phase) and 400 – 600 °C (O-phase) all xyz and Uiso's were refined freely. For mixed phase refinements at 250 – 350 °C, fixed structural models were used, except for refined lattice parameters for each phase. Final refinement details at 100 and 500 °C are given in cif format. Phase evolution versus T is given below:

Table S3. Refined lattice parameters/phase fractions for La_{0.9}Nd_{0.1}TaO₄ versus T, from NPD.

T (°C)	a (Å)	b (Å)	c (Å)	β (deg)	V (Å ³)
100	7.6345(1)	5.5728(1)	7.8181(1)	101.459(1)	326.147(8)
150	7.6368(1)	5.5774(1)	7.8209(1)	101.494(1)	326.445(8)
200	7.6402(1)	5.5805(1)	7.8245(1)	101.544(1)	326.859(8)
250 ^a	7.6435(1)	5.5834(1)	7.8278(1)	101.585(2)	327.261(7)
	3.9384(3)	14.778(1)	5.6284(7)		327.59(4)
300 ^b	7.6460(3)	5.5845(2)	7.8291(2)	101.601(3)	327.47(2)
	3.9392(1)	14.7674(6)	5.6356(2)		327.84(2)
350 ^c	7.6468(9)	5.5839(8)	7.8252(8)	101.57(1)	327.34(5)
	3.9412(1)	14.7471(6)	5.6422(2)		327.94(2)

400	3.94347(8)	14.7119(3)	5.6540(1)		328.02(1)
450	3.94503(6)	14.7044(2)	5.6599(1)		328.33(1)
500	3.94614(5)	14.7058(2)	5.6639(1)		328.69(1)
550	3.94702(5)	14.7096(2)	5.66741(8)		329.047(8)
600	3.94791(4)	14.7152(2)	5.67073(8)		329.438(7)

- a. 90% M, 10% O
- b. 59% M, 41% O
- c. 24% M, 76% O

Figure S3. Rietveld plot for $\text{La}_{0.9}\text{Nd}_{0.1}\text{TaO}_4$ mixed phase (59 % M- plus 41% O-) at 300 °C

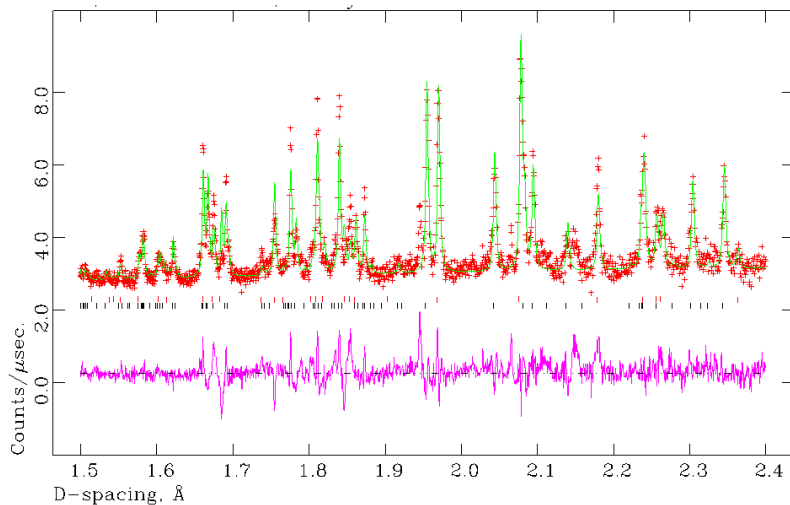


Figure S4. Dielectric data (obtained at various frequencies) as a function of temperature for LaTaO_4 (a) and $\text{La}_{0.90}\text{Nd}_{0.10}\text{TaO}_4$ (b). For clarity only permittivity data at selected frequencies and on heating are presented. The sharp upturn at low frequency and increasing temperature is due to the encroaching grain boundary/electrode polarisation (see e.g., Morrison *et al.*, *J. Appl. Phys.*, 1999, **86** (11), 6355).

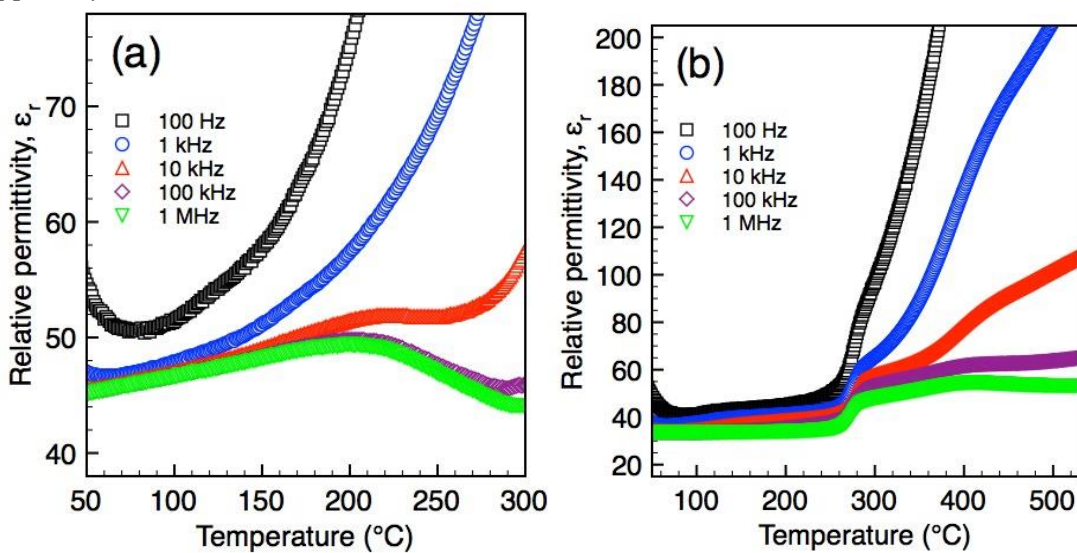


Figure S5. Polarisation-field (P-E) response for O-LaTaO₄ obtained at room temperature, *ca.* 100 kV/cm and at 1 kHz (a), 100 Hz (b), 1 Hz (c) and 0.1 Hz (d). The data indicate a linear (slightly lossy) dielectric response at high frequency, with increasing leakage resulting in increasingly open and rounded loops with decreasing frequency.

